Three-phase numerical modeling for equiaxed solidification of Sn–10 wt.%Pb alloy under forced convection driven by electromagnetic force

T Wang, E Wang, Y. Delannoy, Y. Fautrelle, O. Budenkova

Published after ICASP5-CSSCR5
in
IOP Conf. Series: Materials Science and Engineering 529 (2019) 012030
IOP Publishing
doi:10.1088/1757-899X/529/1/012030

Three-phase numerical modeling for equiaxed solidification of Sn–10 wt.%Pb alloy under forced convection driven by electromagnetic force

T Wang[1,2], E Wang[1] , Y Delannoy[2], Y Fautrelle[2] and O Budenkova[2]

[1] Key Laboratory of Electromagnetic Processing of Materials (Ministry of Education), Northeastern University, P. R. China
[2] Univ. Grenoble Alpes, CNRS, Grenoble INP, SIMAP, F-38000 Grenoble, France
tao.wang1@grenoble-inp.fr

Abstract. A three-phase equiaxed solidification model where macroscale heat transfer and fluid flow are coupled with microscale nucleation and dendrite growth, is applied to the simulation of the macrosegregation in binary alloy solidification subjected to the electromagnetic stirring. The investigated experimental solidification case is conducted in a cavity which has a good control of the thermal boundary conditions. The proposed model uses a double time step scheme to accelerate the solution. Electromagnetic force is introduced as a source term into momentum equation in analytical form. To account for the friction from the side walls, a 2D½ flow model is applied to a three-dimensional experimental configuration. A comparison between the results of simulation and experimental ones is made.

1. Introduction

Macrosegregation defects often appear in ingot especially during a long-time solidification. These defects cannot be removed by the subsequent heat treatment or rolling process, and will affect the product properties. Magnetic fields and electromagnetic force have been widely applied to control solute distribution and grain structure [1–3]. It was shown that using the electromagnetic stirring during solidification, a larger equiaxed grain zone and finer grain size can be obtained and macrosegregation can be reduced [4]. However, sometimes heavier macrosegregation will be generated by the strengthened convection if parameters of electromagnetic stirring (EMS) are not appropriately chosen [3]. It is of high significance to have deep understanding of the mechanism how EMS affects the solute distribution during solidification that can be obtained through dedicated experiment and numerical modelling.

Volume/Statistical average method is a probable way to anticipate segregation formation since it can relate macroscopic variables to the microscopic ones. Various volume-averaged models have been developed aiming predict macrosegregation and solidification structure, including continuum model [5,6], columnar model [7], equiaxed model [8–12] and mixed model [13–16]. In each of them, phases attribution and growth kinetic vary based on different physical assumption.

In order to provide an experimental basis for the validation of numerical simulation, SIMAP/EPM laboratory in France designed a benchmark solidification setup, referred hereafter AFRODITE. The main characteristics of this experiment setup are: (1) controlled thermal boundary conditions (2) real-time whole-field temperature measurements (3) possibility to realize various solidification condition

and (4) possibility to use different modes of EMS during solidification. During solidification, a temperature map is recorded by a lattice of 50 thermocouples. After solidification, the post-mortem analysis of the sample is made regarding the segregation pattern (with X-ray and/or using probes); the grain structures and dendrite parameters. Several experiments have been performed already. First, Wang and Fautrelle [17] carried out solidification experiment on pure tin with natural convection. Then, Hachani and co-workers studied the effect of different initial concentration in solidification of a tin-led alloy with natural convection [18]. The latest results obtained with the AFRODITE set-up were related to the effect of the various modes of the electromagnetic stirring during the solidification of a tin-lead alloy on the segregation and final structure of ingot [19]. Numerical calculations were performed for AFRODITE solidification without EMS using volume and statistical average method in two-dimensional and three-dimensional configurations, using columnar solidification model [20] or mixed columnar-equiaxed solidification model [21]. It was shown that the solidification phenomena have been well repeated through volume averaged method, although some boundary conditions and crucial parameters should be further confirmed.

The objective of current work is to simulate the influence of EMS on the AFRODITE benchmark solidification through a new volume averaged equiaxed solidification model, and compare numerical results with experimental ones. This work focus on the grains' growth and phases' movement and formation of macrosegregation, we do not consider the dendrite break-off phenomenon although it could happen under strong convection.

2. Experimental setup

The concerning experiment is a solidification of Sn–10 wt.%Pb alloy in a rectangular cavity with inside size of 100 × 60 × 10 mm. The temperature of left and right boundary are controlled to keep a difference of 40 K between the thermocouples placed outside of the liquid phase at the heaters, and to cool them down with same rate which for the case under consideration was CR = 0.03 K/s [20], other walls can be regarded as non-slip and adiabatic, In such configuration a natural thermal convection develops in the liquid which drives the latter upward along the hot wall, downward along the cold wall, and consequently, from the hot wall toward the cold wall along the top of the cavity and in the opposite direction along the bottom [20]. To introduce the EMS in the liquid phase, a travelling magnetic field was created with a linear motor placed horizontally along the cavity and below it. In such configuration the Lorentz force acts in the liquid mostly along the bottom and decreases exponentially in the vertical direction. An analytical expression for the resulting Lorentz force can be found elsewhere [22] and was used in the numerical simulations. Hereafter we consider the experiment in which the Lorentz force created the motion of the melt opposite to the one generated by the buoyancy force, the frequency and the intensity of the coil current was 50 Hz and I = 8.2 A, respectively.

More details about the experiment as well as correspond results can been found in the reference [19] for the experimental case number 3. In the work, most material properties are taken from [23]. However, liquid/solid density and electrical conductivity comes from elsewhere as shown in Table 1.

Table 1. Some material properties Sn–10 wt.%Pb alloy.

	Units		Ref.
Reference density(liquid)	$kg\ m^{-3}$	7246	[24]
Solid density	$kg\ m^{-3}$	7199	[24]
Electrical conductivity (liquid)	$Ohm^{-1}cm^{-1}$	2×10^{4}	[25]
Electrical conductivity (solid)	$Ohm^{-1}cm^{-1}$	2.5×10^{4}	[25]

3. Model description and numerical approach

In the numerical simulations, only the equiaxed model is employed, because the post-mortem analysis of the sample solidified under described conditions revealed mostly equiaxed grain structure (see figure 10c in [19]). Similar to [26], [14] and [27], in our model we distinguish three phases : the liquid outside the envelope of equiaxed dendrite (l-phase), the interdendritic liquid (d-phase) and the solid dendrite (s-phase) that gives the corresponding fractions $f_d + f_s + f_l = 1$. Lipton–Glicksman–Kurz (LGK) tip growth kinetics is applied to estimate the evolution of the grain envelope. The solidification of interdendritic melt is driven by the difference between equilibrium liquid concentration and interdendritic liquid concentration. The solute diffusion equation around the growing grains' envelope is calculated according to [12], in which the diffusion length l_{ld} considered the influence of growth status, grain's size and fluid flow as:

$$l_{ld} = \min\left(\frac{D_l}{v_{en}}, \frac{d_{eq}}{Sh}\right)$$

Where v_{en} is envelope growth velocity, d_{eq} is the average grains' diameter, Sh is Sherwood number accounting for the effect of fluid flow on grains's movement.

Considering that temperature varies in the cavity, a simple melting model [28] was included. Other details about the grain growth model and macroscopic conservation omitted here because of brevity are similar to the ones in [27].

In terms of momentum transport, s-phase and d-phase are treated as union, which is literally the dendritic structure of an equiaxed grain (e-phase), whose fraction is $f_e = f_d + f_s$, respectively. This means also that the interdendritic liquid and solid dendrite share the same velocity field while the velocity of the extradendrite liquid is different. The momentum exchange between the grain and the liquid phase is accounted for with a drag model proposed in [29] (equation (26) and Table I) The flow partitioning effect between the interdendritic and extradendritic liquid is neglected for simplicity. When $f_e \geq f_e^c$, the grain phase is packed, i.e. it becomes immovable while the permeability of the grain fraction is changed and is calculated with Carman-Kozeny equation based on a constant characteristic length number related to grains' density. Nucleation happens in extradendritic liquid immediately when the alloy temperature is lower than liquidus temperature. Nuclei density is defined as a scalar and move with grain phase.

In our approach the processes which occur at macroscopic and microscopic scale are modelled with different time steps. A larger time step is used for the calculation of the transport phenomena at the macro-sale and a smaller time sub-steps is used for the calculation of the processes within the grain (diffusion, solidification) and the grain growth. The macroscopic calculation, including multiphase flow field and transport of energy, solute and nuclei density, are solved by ANSYS FLUENT® software in which the modeling of the solidification at the microscale is implemented with user-defined functions.

4. Results and discussion

The AFRODITE experiment is supposed to be a quasi-2D benchmark although the thickness of the cavity is only 10mm that affects strongly the flow. Yet, the two-dimensional simulation of the experiment is still possible if an additional source term is introduced into the momentum equations to take into account the frictions from the large lateral walls which are absent in two-dimensional problem statement [30]. In the present simulation this term was implemented in the momentum equation for the liquid phase as well as the analytical expression for the Lorentz force. Similar to the previous simulations, it is supposed that the temperature difference between the cold and the hot boundaries is less than those seen on the external thermocouples because of a thermal resistance. Based on the temperature distributions in liquid [21] we estimated this difference around 15 degrees which was used in the simulations.

The preliminary simulations of the melt flow performed with laminar approach did not converge. It was found that the motion caused by the EMS force overcomes the buoyancy convection at the bottom and near the cold wall of the cavity. However, the upward flow near the hot wall remains and interaction of two vortices near the cavity center causes flow instabilities. Consequently, for further simulations a

RNG k-e turbulent model was used. It should be noted that the calculated turbulent viscosity was rather weak.

As shown in table 1, for Sn–10 wt.%Pb alloy electrical conductivity of the solid is larger than the liquid one [25], therefore, the Lorentz force acting on grain phase has to be taken into account proportionally to the solid fraction. At the beginning of solidification, the Lorentz force acting on grains does not have crucial effect because solid fraction is still low. This force will be important when the grain phase is going to be packed. The force on solid could strength the melt flow via drag force and retard the grain packing phenomenon.

The temperature distributions after 50s of solidification (figure 1b) is quite similar to the one observed in the experiment and two vortices described above exist in the liquid. The maximum liquid velocity is 3.48 cm/s which corresponds to experimental estimations [19] and to the Reynolds number Re=4307, i.e. to a transition regime or a weakly turbulent flow. At this stage the grain phase prefers to nuclei and grow first at upper right corner, where has lowest temperature in cavity because the liquid flow upwards at this cold side. Some grains remain at the corner and further grow up while others flow into bulk liquid and then remelt gradually.

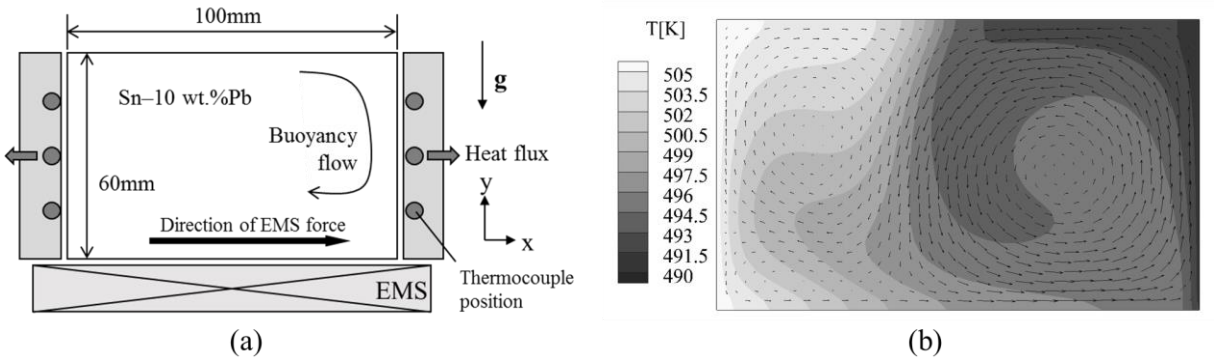

Figure 1. Experiment schedule (a); Temperature distribution and averaged velocity distribution at 200s ($\left|\langle \vec{v}_{average} \rangle\right|_{max} = 34.8$ mm/s) (b).

At 540s, two vortexes with different direction still persist in the cavity, yet, the vortex generated by EMS force is located only at a lower part of the cavity. Another vortex forms because of the thermal-solute effect, which become pronounced with rejection of Pb during solidification. These two flows collide near the center of hot wall and then separate. Both vortices bring some unmelted grains back to the cold region and attend solidification again. However, another factor which is important to the grain distribution is the density. According to the chosen properties, the density of the solid phase is constant and larger than the density of the liquid if the concentration of Pb in liquid is less than about 8.7wt%, depending also on temperature. The upper flow will take the grains to the top region, some grains can remain at top because they are lighter than liquid thus forms negative segregation region. At grain faction $f_e = f_e^c$, the grain phase velocity vanish while liquid flow become weak in this region due to rapidly increasing flow resistance. The packed grains layer which is poorer in Pb first form at right wall then gradually extend leftwards. Because of the EMS force driving flow, there is a thicker equiaxed grain layer at top rather than bottom.

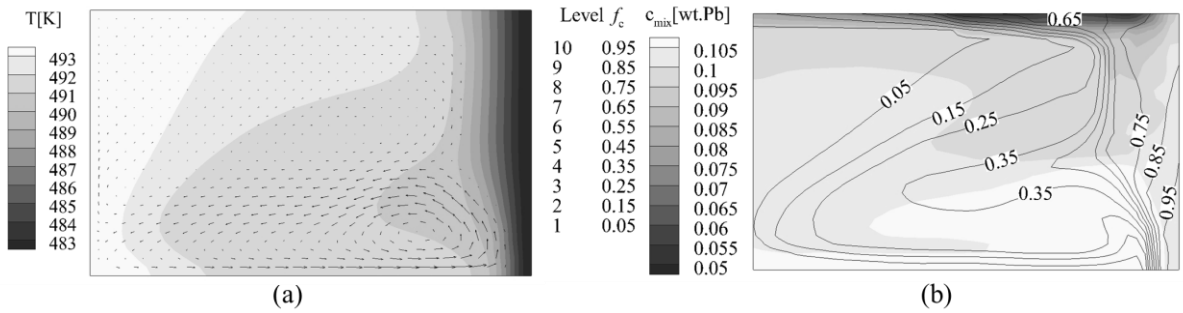

Figure 2. Temperature distribution and averaged velocity distribution at 540s ($\left|\langle \vec{v}_{average} \rangle\right|_{max}$ = 24.1 mm/s) (a); concentration and grain fraction distribution at 540s (b).

After 900s, almost whole the cavity except the bottom layer is filled by the packed grain and become rigid. Minor flow still exists at bottom layer because the liquid is highly enriched and will solidify later when the temperature becomes lower than local liquidus temperature, or eutectic temperature. The maximum value of liquid velocity in the layer is only 1.41 mm/s, and has negligible influence on concentration transport.

Final macrosegregation map is shown in figure 3. A positive segregation zone forms from the central bottom and seems flow towards upper rightwards, which is quite similar to the experimental results (see figure 12c in [19]). This happens because the flow driven by EMS brings enriched liquid rightwards at the bottom of cavity. The enriched flow turns upwards when being blocked by packed grains layer at right side. A slightly negative segregated layer at the top is also predicted, and is formed because of two reason. Firstly, some unmelted grains stay at the top because they have lighter density than liquid, they will continue to grow if temperature is lower than liquidus temperature. Secondly, Pb rejected from solid during solidification will enrich liquid phase thus give it higher density. The enriched liquid tends to flow downwards and will be replenish by fresh alloy from bulk liquid. However, the segregation channel at right lower corner is not repeated maybe it involves the columnar grain structure, which are not included in current research.

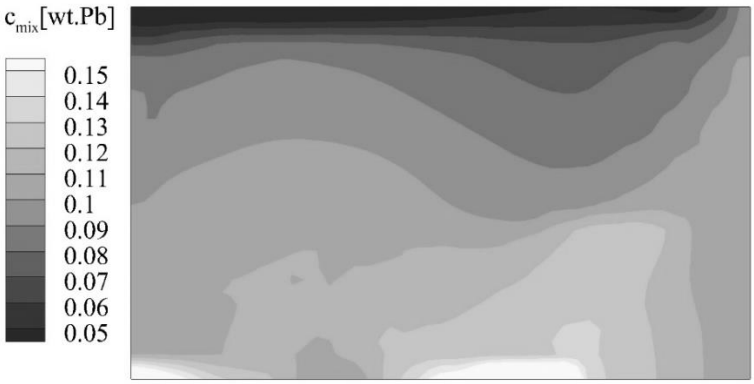

Figure 3. Macrosegregation map obtained from calculation at 1440s.

5. Summary

A 3-phase equiaxed solidification model is applied in predicting the AFRODITE experiment for Sn–10 wt.%Pb alloy under the forced convective flow driven by EMS. The grain fraction distribution, liquid flow field and macrosegregation map have been presented and analyzed. The result shows that the applied EMS force can change the flow motion at bottom of cavity. Strong EMS driving flow bring more unpacked grains from solidification frontier to the bulk liquid. The stirring has effect of enlarging

the isothermal region. Calculated macrosegregation map shows similar negative segregated layer at top and positive segregation zone at bottom as experimental one.

Acknowledgements
This work is a joint cooperation between SIMAP laboratory of Grenoble INP (France) and Key Laboratory of EPM of Northeastern University (P. R. China). The authors gratefully acknowledge financial support from China Scholarship Council (No. 201706080074), National Key R&D Program of China (Grant No. 2017YFE0107900) and National Nature Science Foundation of China (Grant No. U1760206). The SIMAP laboratory acknowledges the financial support through ESA-MAP MICAST project contract 14347/01/NL/SH.

References
[1] Spitzer K-H, Reiter G and Schwerdtfeger K 1996 ISIJ Int. 36 487–92
[2] Tzavaras A A and Brody H D 1984 JOM J. Miner. Met. Mater. Soc. 36 31–7
[3] Medina M, Du Terrail Y, Durand F and Fautrelle Y 2004 Metall. Mater. Trans. B Process Metall. Mater. Process. Sci. 35 743–54
[4] Campanella T, Charbon C and Rappaz M 2004 Metall. Mater. Trans. A Phys. Metall. Mater. Sci. 35 A 3201–10
[5] Plotkowski A and Krane M J M 2016 Comput. Mater. Sci. 124 238–48
[6] Bennon W D and Incropera F P 1988 Numer. Heat Transf. 13 277–96
[7] Bellet M, Combeau H, Fautrelle Y, Gobin D, Rady M, Arquis E, Budenkova O, Dussoubs B, Duterrail Y, Kumar A, Gandin C A, Goyeau B, Mosbah S and Založnik M 2009 Int. J. Therm. Sci. 48 2013–6
[8] Wu M and Ludwig A 2009 Acta Mater. 57 5621–31
[9] Ni J and Beckermann C 1993 J. Mater. Process. Manuf. Sci. 2 217–31
[10] Založnik M and Combeau H 2010 Comput. Mater. Sci. 48 1–10
[11] Wang C Y and Beckermann C 1996 Metall. Mater. Trans. A 27 2754–64
[12] Appolaire B, Combeau H and Lesoult G 2008 Mater. Sci. Eng. A 487 33–45
[13] Wu M, Fjeld A and Ludwig A 2010 Comput. Mater. Sci. 50 32–42
[14] Ciobanas A I and Fautrelle Y 2007 J. Phys. D. Appl. Phys. 40 3733–62
[15] Ciobanas A I and Fautrelle Y 2007 J. Phys. D. Appl. Phys. 40 4310
[16] Silva J N, Moutinho D J, Moreira A L, Ferreira I L and Rocha O L 2009 J. Alloys Compd. 478 358–66
[17] Wang X and Fautrelle Y 2009 Int. J. Heat Mass Transf. 52 5624–33
[18] Hachani L, Zaidat K, Saadi B, Wang X D and Fautrelle Y 2015 Int. J. Therm. Sci. 91 34–48
[19] Hachani L, Zaidat K and Fautrelle Y 2015 Int. J. Heat Mass Transf. 85 438–54
[20] Boussaa R, Hachani L, Budenkova O, Botton V, Henry D, Zaidat K, Ben Hadid H and Fautrelle Y 2016 Int. J. Heat Mass Transf. 100 680–90
[21] Zheng Y, Wu M, Karimi-Sibaki E, Kharicha A and Ludwig A 2018 Int. J. Heat Mass Transf. 122 939–53
[22] Wang X, Moreau R, Etay J and Fautrelle Y 2009 Metall. Mater. Trans. B 40 104–13
[23] Založnik M, Kumar A and Combeau H 2010 Comput. Mater. Sci. 48 11–21
[24] Stankus S V. and Khairulin R A 2006 High Temp. 44 389–95
[25] Plevachuk Y, Sklyarchuk V, Yakymovych A, Willers B and Eckert S 2005 J. Alloys Compd. 394 63–8
[26] Wang C Y and Beckermann C 1993 Metall. Trans. A 24 2787–802
[27] Wu M and Ludwig A 2009 Acta Mater. 57 5632–44
[28] Ludwig A and Wu M 2002 Metall. Mater. Trans. A 33 3673–83
[29] Wang C Y, Ahuja S, Beckermann C and de Groh H C 1995 Metall. Mater. Trans. B 26 111–9
[30] Botton V, Boussaa R, Debacque R, Hachani L, Zaidat K, Ben Hadid H, Fautrelle Y and Henry D 2013 Int. J. Therm. Sci. 71 53–60